Effects of CT and VT Connection Point on Distance Protection of Transmission Lines with FACTS Devices

H. Shateri* and S. Jamali*

Abstract: This paper presents the effects of instrument transformers connection points on the measured impedance by distance relays in the presence of Flexible Alternating Current Transmission System (FACTS) devices with series connected branch. Distance relay tripping characteristic itself depends on the power system structural conditions, pre-fault operational conditions, and especially the ground fault resistance. The structural and controlling parameters of FACTS devices as well as the connection points of instrument transformers affect the ideal tripping characteristic of distance relay. This paper presents a general set of equations to evaluate the measured impedance at the relaying point for a general model of FACTS devices to consider different affecting parameters.

Keywords: Distance protection, Fault resistance, FACTS devices, Tripping characteristic.

1 Introduction

The measured impedance at the relaying point is the basis of the distance protection operation. There are several factors affecting the measured impedance at the relaying point. Some of these factors are related to the power system parameters prior to the fault instance, which can be categorized into two groups. First group is the structural conditions, while the second group is the operational conditions [1-3]. In addition to the power system parameters, the fault resistance, in the single-phase to ground faults, could greatly influence the measured impedance, in such a way that for zero fault resistance, the power system parameters do not affect the measured impedance. In other words, power system parameters affect the measured impedance only in the presence of the fault resistance, and as the fault resistance increases, the impact of power system parameters becomes more severe.

In the recent years FACTS devices are introduced to the power systems to increase the transmitting capacity of the lines and provide the optimum utilization of the system capability. This is done by pushing the power systems to their limits. It is well documented in the literature that the introduction of FACTS devices in power systems has a great influence on their dynamics. As power system dynamics changes, many sub-systems are affected, including the protective systems. Therefore, it is essential to study effects of FACTS devices on the protective systems, especially the distance protection, which is the main protective device at UHV, EHV, and HV levels.

Unlike power system parameters, the structural and controlling parameters of FACTS devices could affect the measured impedance even in the absence of the fault resistance. In the presence of FACTS devices, the conventional distance characteristic such as Mho and Quadrilateral are greatly subjected to mal-operation in the form of over-reaching or under-reaching the fault point.

Regarding the high levels of currents and voltages in the UHV, EHV, and HV systems, it is essential to provide the current and voltage signals for the protective system via the instrument transformers. In the presence of FACTS devices at the near end of the line, the connection points of the Voltage Transformers (VT) and/or the Current Transformer (CT) can be either behind or in front of these devices. As the connection points changes, considerable variations in the measured impedance could be resulted.

Reference [4] has presented the measured impedance at the relaying point in the presence of UPFC on a single circuit line, and [5] has presented the measured impedance in the presence of series connected FACTS devices (TCSC, TCPST, and UPFC) on a double circuit line. The importance of instrument transformers connection points on distance relays performance has been mentioned in [6-7] for TCSC and in [8] for UPFC. References [6-8] has discussed the effect of FACTS devices by means of simulation or simple symbolic equations, and unlike [4-5] has not presented the detailed accurate equations. The effects of the instrument transformers connection points have been

Iranian Journal of Electrical & Electronic Engineering, 2006.
* The authors are with the Center of Excellence for Power Systems Automation and Operation, Department of Electrical Engineering, Iran University of Science and Technology, Narmak, Tehran 16846, Iran.
E-mail: shateri@iust.ac.ir, sjamali@iust.ac.ir.

studied for TCSC in [9], for UPFC in [10], and for SSSC in [11] by means of presenting the measured impedance at the relaying point in the case of the various instrument transformers connection points. In [9-11] the effects of the instrument transformers connection points have been presented for each device individually. This paper intends to study the effects of the instrument transformers connection points generally by means of considering the general model for all of the concerning FACTS devices and presenting the generalized equations for the measured impedance.

The measured impedance at the relaying point in the presence of FACTS devices with series connected branch, including TCSC, SSSC, TCPST, UPFC, at the near end of the line for different distance relay instrument transformers connection points. This is done by presenting the general equations set for the general model of FACTS devices. Regarding the presented measured impedance and the tripping characteristic, it can be seen how much a distance relay is sensitive to its instrument transformers connection points in the presence of FACTS devices with series branch at the near end of the line.

2 Modeling FACTS Devices

As mentioned, FACTS devices with series connected branch, including TCSC, SSSC, TCPST, UPFC, are studied here. The model of each of these devices and the general model for these devices are presented in this section.

2.1 TCSC

Thyristor Controlled Series Compensator (TCSC) consists of a fixed capacitor in parallel with a thyristor controlled reactor [7,12]. TCSC can be controlled by adjusting the conducting duration of the reactor. TCSC can be modeled as a variable reactance, capacitive or inductive, regarding the conducting duration of the thyristors, the inductance of the rector, and the capacitance of the capacitor, as it is shown in Fig. 1. The reactance of TCSC is usually defined as the per unit of the positive sequence impedance of the transmission line, which is given as TCSC compensation degree, K_C, as below:

$$Z_{TCSC} = -jK_C X_{1L} \qquad (1)$$

2.2 SSSC

Static Synchronous Series Compensator (SSSC) is placed in the group of series connected FACTS devices. SSSC consists of a voltage source inverter connected in series via a coupling transformer to the transmission line. A source of energy is required for providing and maintaining the dc voltage across the dc capacitor and compensation of SSSC losses [12].

Figure 2 shows the model of SSSC which consists of a series connected voltage source in series with an impedance. This impedance represents the impedance of SSSC coupling transformer.

When the energy source only has the ability of maintaining the dc voltage and supplying the losses, SSSC only could compensate the reactive power. In this case the magnitude of injected voltage can be controlled due to compensation strategy, but the phase angle of the injected voltage would be perpendicular to the line current. The injected voltage could either lead or lag the line current by 90°.

2.3 TCPST

Thyristor Controlled Phase Shifter Transformer (TCPST) consists of two transformers, magnetizing and booster transformers, which are connected through a thyristor switching device [7,12]. Magnetizing transformer is the shunt connected transformer while the booster transformer is connected in series with the transmission line. The injected voltage via the booster transformer is perpendicular to the input voltage of TCPST.

The equivalent circuit of TCPST is shown in Fig. 3. This model consists of two branches, a shunt and a series branch. The shunt branch is related to the magnetizing transformer, which is presented by the magnetizing transformer impedance, Z_{Sh}, and its voltage, E_{Sh}. The series branch is corresponding to the boosting transformer, which is represented by the booster transformer impedance, Z_{Se}, and its series injected voltage $re^{j\theta} V_i$.

The parameters of the series branch, r and θ, could be represented according to the phase angle shifting, φ, as:

$$r = \tan(|\varphi|) \qquad (2)$$

$$\theta = \text{sign}(\varphi)\ \pi/2 \qquad (3)$$

Fig. 1 Equivalent circuit (model) of TCSC.

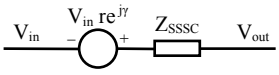

Fig. 2 Equivalent circuit (model) of SSSC.

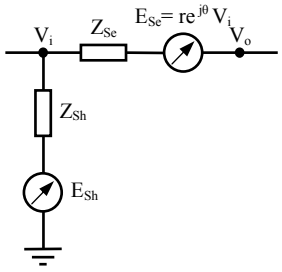

Fig. 3 Equivalent circuit (model) of TCPST.

2.4 UPFC

Unified Power Flow Controller (UPFC) consists of two converters, series and shunt connected converters to the transmission line, which have a common dc link via a dc storage capacitor [8,12]. The shunt connected converter inject or absorb the reactive power and provide the required active power of the series converter. The series connected converter injects a variable voltage, in the form of both variable magnitude and phase angle. These converters are operating independently from the reactive power point of view, but the required active power of series connected converter, and the losses of both converters and storage capacitor, is provided via the shunt connected converter. The equivalent circuit of UPFC is the same as that is shown in Fig. 3, which consists of two branches, a shunt and a series branch, the same as TCPST. The shunt branch is related to the shunt connected converter, which is presented by the impedance Z_{Sh} and the voltage source E_{Sh}. The series branch is corresponding to the series connected converter; and is represented by the impedance Z_{Se} and the voltage source $re^{j\theta} V_i$.

2.5 General Model

The model of Fig. 3 could be utilized as the general model for FACTS devices. The model of TCPST and UPFC are just the same as Fig. 3. In the case of SSSC, if the impedance of the shunt branch becomes infinite, the model of SSSC would be resulted. For TCSC, if the impedance of the shunt branch becomes infinite and r becomes zero, the model of TCSC would be the result. The parameters of the general model for each of FACTS devices are presented in Table 1.

Table 1 General model for FACTS devices.

	Z_{Sh}	E_{Sh}	Z_{Se}	r	θ
TCSC	∞	--	Z_{TCSC}	0	--
SSSC	∞	--	Z_{SSSC}	r	θ
TCPST	Z_{Sh}	E_{Sh}	Z_{Se}	r	θ
UPFC	Z_{Sh}	E_{Sh}	Z_{Se}	r	θ

3 Measured Impedance at Relaying Point

Distance relays operate based on the measured impedance at the relaying point. In the absence of FACTS devices and for zero fault resistance, the measured impedance by a distance relay only depends on the length of the line section between the fault and the relaying points. In Fig. 4 this impedance is equal to pZ_{1L}, where p is per unit length of the line section lied between the fault and the relaying points, and Z_{1L} is the line positive sequence impedance in ohms.

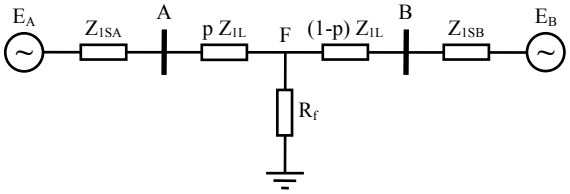

Fig. 4 Equivalent circuit for single phase to ground fault.

In the case of a non-zero fault resistance, the measured impedance is not equal to the impedance of the line section located between the relaying and fault points. In this case, the structural and operational conditions of the power system affect the measured impedance. The structural conditions are evaluated by the short circuit levels at the line ends, S_{SA} and S_{SB}. The operational conditions prior to the fault instance can be represented by the load angle of the line, δ, and the ratio of the voltage magnitude at the line ends, h, or in general $E_B / E_A = he^{-j\delta}$. In the absence of FACTS devices and with respect to Fig. 4 and Fig. 5, the measured impedance can be expressed by the following equations. More detailed calculations can be found in [2].

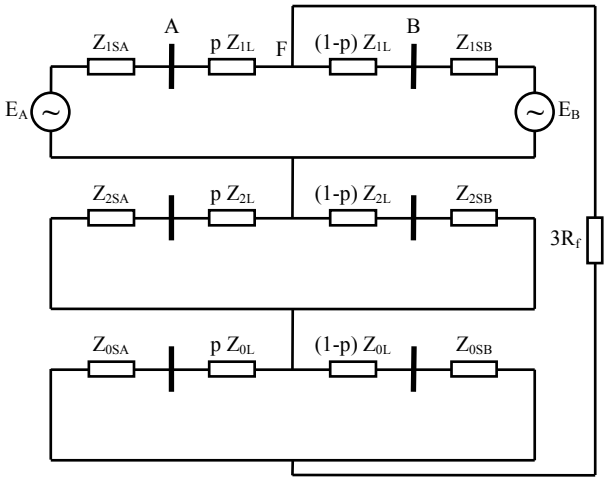

Fig. 5 Equivalent circuit of phase A to ground fault.

$$Z_{1A} = Z_{1SA} + pZ_{1L} \tag{4}$$

$$Z_{1B} = Z_{1SB} + (1-p)Z_{1L} \tag{5}$$

$$Z_{0A} = Z_{0SA} + pZ_{0L} \tag{6}$$

$$Z_{0B} = Z_{0SB} + (1-p)Z_{0L} \tag{7}$$

$$Z_{\Sigma} = 2\frac{Z_{1A}Z_{1B}}{Z_{1A}+Z_{1B}} + \frac{Z_{0A}Z_{0B}}{Z_{0A}+Z_{0B}} \tag{8}$$

$$C_1 = \frac{Z_{1B}}{Z_{1A}+Z_{1B}} \tag{9}$$

$$C_0 = \frac{Z_{0B}}{Z_{0A}+Z_{0B}} \tag{10}$$

$$K_{0L} = \frac{Z_{0L}-Z_{1L}}{3Z_{1L}} \tag{11}$$

$$K_{ld} = \frac{1-he^{-j\delta}}{Z_{1A}he^{-j\delta}+Z_{1B}} \tag{12}$$

$$C_{ld} = (Z_{\Sigma} + 3R_f)K_{ld} \tag{13}$$

$$Z_A = p\,Z_{1L} + \frac{3R_f}{C_{ld} + 2C_1 + C_0(1+3K_{0L})} \tag{14}$$

It can be seen for zero fault resistance, the measured impedance at the relaying point is the impedance of the line section between the relaying and the fault points. The power system conditions only affect the measured impedance in the presence of the fault resistance.

In the presence of FACTS devices at the near end of the line, as shown in Fig. 6, four different cases could be considered due to the CT and VT connection points.

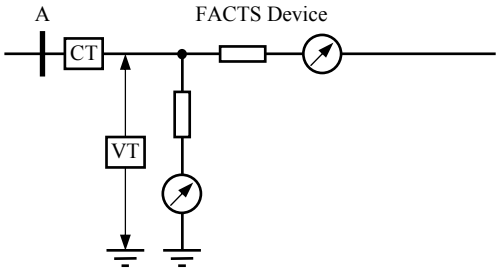

a) VT behind, CT behind FACTS device

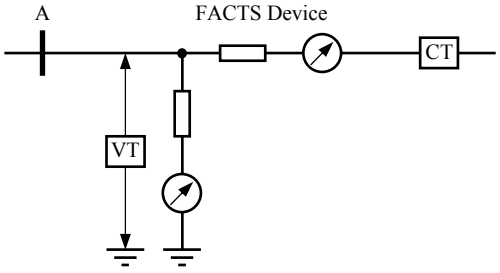

b) VT behind, CT in front of FACTS device

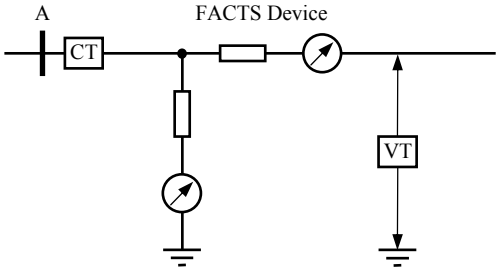

c) VT in front of, CT behind FACTS device

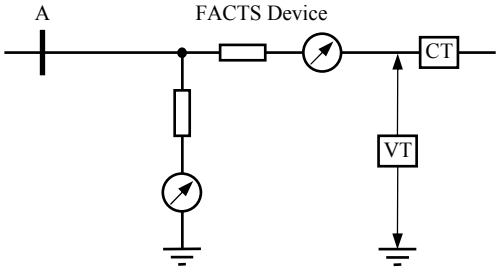

d) VT in front of, CT in front of FACTS device

Fig. 6 Various CT and VT connection points.

Once FACTS devices are installed at the near end of the line, (4), (6), (12), and (13) should be modified and some new equations are introduced:

$$C_{1S} = \frac{Z_{Se}}{Z_{1L}} \tag{15}$$

$$C_{0S} = \frac{Z_{Se}}{Z_{0L}} \tag{16}$$

$$Z_{1AI} = Z_{1SA} \tag{17}$$

$$Z_{1AF} = (p + C_{1S})Z_{1L} \tag{18}$$

$$Z_{1BF} = Z_{1SB} + (1-p)Z_{1L} \tag{19}$$

$$Z_{1BI} = Z_{1SB} + (1+C_{1S})Z_{1L} \tag{20}$$

$$Z_{0AI} = Z_{0SA} \tag{21}$$

$$Z_{0AF} = (p + C_{0S})Z_{0L} \tag{22}$$

$$Z_{1A} = Z_{1AF} + \frac{Z_{Sh}Z_{1AI}}{Z_{Sh} + Z_{1AI}} \tag{23}$$

$$Z_{0A} = Z_{0AF} + \frac{Z_{Sh}Z_{0AI}}{Z_{Sh} + Z_{0AI}} \tag{24}$$

$$C_{1A} = \frac{Z_{Sh}}{Z_{Sh} + Z_{1AI}} \tag{25}$$

$$C_{0A} = \frac{Z_{Sh}}{Z_{Sh} + Z_{0AI}} \tag{26}$$

$$\begin{aligned} Den = {} & Z_{1AI}[Z_{1AF}he^{-j\delta} + Z_{1BF}(1+re^{j\theta})E_{Sh}] \\ & + Z_{Sh}\begin{bmatrix}[Z_{1AI}(1+re^{j\theta}) + Z_{1AF}]he^{-j\delta} \\ + Z_{1BF}(1+re^{j\theta})\end{bmatrix} \end{aligned} \tag{27}$$

$$\begin{aligned} K_{ld_\Delta} = {} & Z_{1AI}[(1+re^{j\theta})E_{Sh} - he^{-j\delta}] \\ & - Z_{1BI}[1-E_{Sh}] \end{aligned} \tag{28}$$

$$C_{ld_\Delta} = (Z_{\Sigma} + 3R_f)K_{ld_\Delta} / Den \tag{29}$$

$$C_{Sh} = Z_{1AF}\begin{bmatrix}C_{ld_\Delta} + 2C_1(1-C_{1A}) \\ + C_0(1-C_{0A})(1+3K_{0L})\end{bmatrix} \tag{30}$$

$$C_{Z_{Se}} = (C_{0S} - C_{1S})(1+3K_{0L})C_0 Z_{1L} \tag{31}$$

$$K_{V_{Se}} = Z_{1AI}Z_{1BI}E_{Sh} + Z_{Sh}[Z_{1AI}he^{-j\delta} + Z_{1BI}] \quad (32)$$

$$C_{V_{Se}} = -(Z_{\Sigma} + 3R_f)K_{V_{Se}}re^{j\theta} / Den \quad (33)$$

$$K_{ld_b} = Z_{1BI}[1 - E_{Sh}] + Z_{Sh}[1 + re^{j\theta} - he^{-j\delta}] \quad (34)$$

$$C_{ld_b} = (Z_{\Sigma} + 3R_f)K_{ld_b} / Den \quad (35)$$

$$K_{ld_f} = Z_{1AI}[(1 + re^{j\theta})E_{Sh} - he^{-j\delta}] + Z_{Sh}[1 + re^{j\theta} - he^{-j\delta}] \quad (36)$$

$$C_{ld_f} = (Z_{\Sigma} + 3R_f)K_{ld_b} / Den \quad (37)$$

Depending on the instrument transformers connection points, (14) should be modified.
In the case of VT behind and CT behind the device:

$$Z_A = (p + C_{1S})Z_{1L} + \frac{C_{Sh} + C_{Z_{Se}} + C_{V_{Se}} + 3R_f}{C_{ld_b} + 2C_1C_{1A} + C_0C_{0A}(1 + 3K_{0L})} \quad (38)$$

In the case of VT behind and CT in front of the device:

$$Z_A = (p + C_{1S})Z_{1L} + \frac{C_{Z_{Se}} + C_{V_{Se}} + 3R_f}{C_{ld_f} + 2C_1 + C_0(1 + 3K_{0L})} \quad (39)$$

In the case of VT in front of and CT behind the device:

$$Z_A = pZ_{1L} + \frac{C_{Sh} + 3R_f}{C_{ld_b} + 2C_1C_{1A} + C_0C_{0A}(1 + 3K_{0L})} \quad (40)$$

In the case of VT in front of and CT in front of the device:

$$Z_A = pZ_{1L} + \frac{3R_f}{C_{ld_f} + 2C_1 + C_0(1 + 3K_{0L})} \quad (41)$$

Since (38) to (41) are calculated based on the general model of FACTS devices, these equations could be used for each of the mentioned FACTS devices.
As mentioned, TCPST injects a series voltage which is perpendicular to its input voltage and it leads or lags the input voltage. On the other hand, UPFC injects a series voltage with the variable magnitude and phase angle. Therefore, studies about UPFC will cover cases concerning with TCPST. So here TCPST has not be studied individually.

4 Distance Relay Ideal Tripping Characteristic in Presence of TCSC

The impacts of the installation of TCSC on a transmission line have been tested for a practical system. A 400 kV Iranian transmission line with the length of 300 km has been used for this study. The structure of this line is shown in [13]. By utilizing the Electro-Magnetic Transient Program (EMTP) [14] various sequence impedances of the line are evaluated according to its physical dimensions. The calculated impedances and the other parameters of the system are:
Z_{1L} = 0.01133 + j 0.3037 Ω/km
Z_{0L} = 0.1535 + j 1.1478 Ω/km
Z_{1SA} = 0.6972 + j 7.9696 Ω
Z_{0SA} = 3.1058 + j 11.5911 Ω
Z_{1SB} = 1.3945 + j 15.9391 Ω
Z_{0SB} = 6.2117 + j 23.1822 Ω
h = 0.96
δ = 16º
In the absence of FACTS devices, Fig. 7 shows the ideal tripping characteristic of the distance relay which is the measured impedance at the relaying point as the fault resistance varies from 0 to 200 ohms, while the fault location changes from the relaying point up to the far end of the transmission line.
Due to the absence of the shunt branch in TCSC, the connection point of CT is not important from measured impedance point of view. Therefore, four mentioned cases are reduced into two cases. Here, two cases of VT behind and in front of TCSC are studied.

4.1 VT behind TCSC

In the case of TCSC, due to the absence of the shunt branch or infinite Z_{Sh}, coefficients C_{1A} and C_{0A} are equal to 1; and C_{ldf} and C_{ldb} are equal and they are represented with C_{ld}. On the other hand, series voltage source is zero; therefore, both (38) and (39) are simplified as:

$$Z_A = (p + C_{1S})Z_{1L} + \frac{C_{Z_{Se}} + 3R_f}{C_{ld} + 2C_1 + C_0(1 + 3K_{0L})} \quad (42)$$

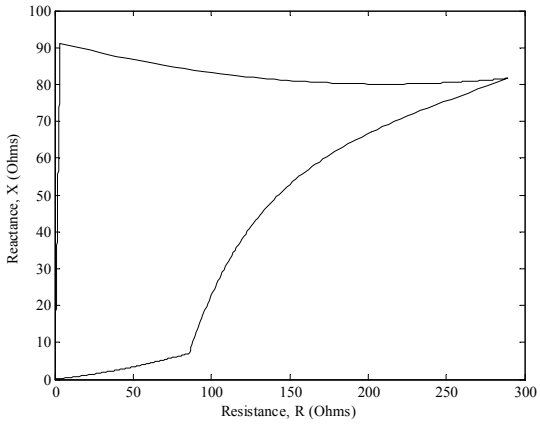

Fig. 7 Distance relay tripping characteristic; without FACTS devices.

The effect of an inactive TCSC presence on the line could be seen in Fig. 7. Here, the compensation degree is zero and TCSC does not inject or absorb any reactive power. It can be seen that inactive TCSC does not affect the measured impedance at the relaying point.

Figure 8 shows the impact of TCSC compensation degree variation on the measured impedance at the relaying point. Here, K_C takes the values 0.3, 0.2, 0.1, 0.0, and –0.1. The negative value of compensation degree represents the inductive mode of TCSC.

It can be seen that as the compensation degree increases, the measured resistance decreases, otherwise, in the inductive mode the measured resistance increases. On the other hand, as the compensation degree increases, the tripping characteristic transfers downwards, and in the inductive mode the tripping characteristic transfers upwards. The magnitude of the tipping characteristic transfer is proportional to TCSC equivalent reactance. As the compensation degree increases, the tripping characteristic shrinks horizontally and transfers downwards.

4.2 VT in front of TCSC

In the case of TCSC, due to the absence of shunt branch, unit C_{1A} and C_{0A}, equality of C_{ldf} and C_{ldb} to C_{ld}, and the absence of series voltage source, both (40) and (41) are simplified as:

$$Z_A = p\,Z_{1L} + \frac{3R_f}{C_{ld} + 2C_1 + C_0(1+3K_{0L})} \qquad (43)$$

The effect of an inactive TCSC presence on the line could be seen in Fig 7. It can be seen that inactive TCSC does not affect the measured impedance at the relaying point.

Figure 9 shows the impact of TCSC compensation degree variation on the measured impedance at the relaying point. Here, K_C takes the values 0.3, 0.2, 0.1, 0.0, and –0.1, the same as Fig. 8.

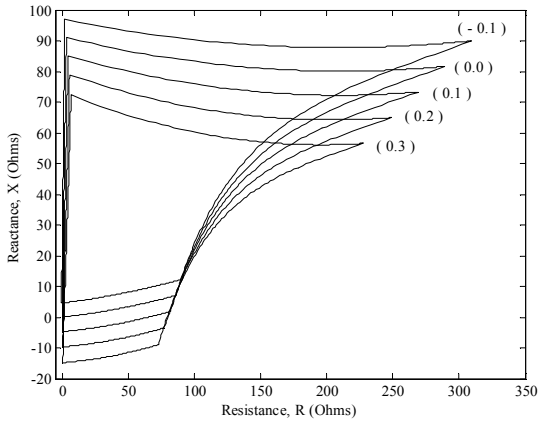

Fig. 8 Distance relay tripping characteristic variation; VT behind TCSC.

In this case, like the previous case, it can be seen that as the compensation degree increases, the measured resistance decreases, otherwise, in the case of TCSC in the inductive mode the measured resistance increases. As the compensation degree increases, the measured reactance does not vary considerably, in both inductive and capacitive modes. In this case, as the compensation degree increases, the tripping characteristic approaches the reactance axis (shrinks), on the other hand for the inductive compensation, the tripping characteristic expands and the measured impedance deviates more than the case without TCSC installation on the line.

5 Distance Relay Ideal Tripping Characteristic in Presence of SSSC

Due to the absence of the shunt branch in SSSC, the same as TCSC, the connection point of CT is not important. Therefore, two cases of VT behind and in front of SSSC are studied.

5.1 VT behind SSSC

In the case of SSSC, due to the absence of shunt branch, unit C_{1A} and C_{0A}, and equality of C_{ldf} and C_{ldb} to C_{ld}, both (38) and (39) are simplified as:

$$Z_A = (p + C_{1S})\,Z_{1L} + \frac{C_{Z_{Se}} + C_{V_{Se}} + 3R_f}{C_{ld} + 2C_1 + C_0(1+3K_{0L})} \qquad (44)$$

Figure 10 shows the effect of an inactive SSSC presence on the line. Here, injected voltage of SSSC is zero and it does not inject or absorb any reactive power. The tripping characteristic without SSSC is also shown in dotted form for comparison.

It can be seen that even in the case of an inactive SSSC, i.e. its injected voltage is zero, it would affect the measured impedance at the relaying point. This is due to the presence of the coupling transformer in series with the line. It can be seen that the tripping characteristic expands slightly and transfers upward. The measured resistance increases as well as the measured reactance.

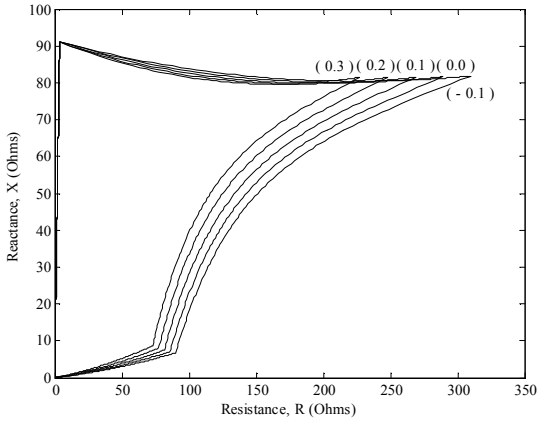

Fig. 9 Distance relay tripping characteristic variation; VT in front of TCSC.

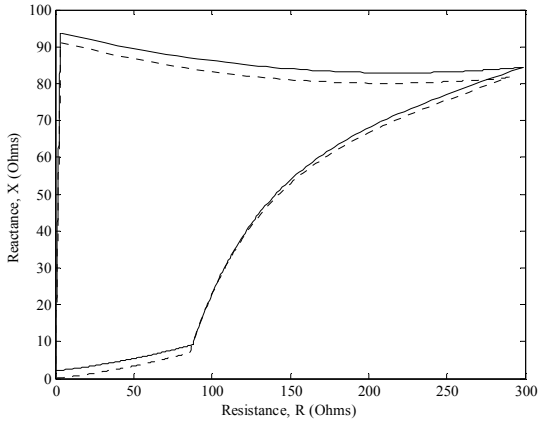

Fig. 10 Distance relay tripping characteristic; VT behind SSSC, inactive SSSC.

Figure 11 shows the effect of SSSC voltage magnitude variation on the measured impedance in the both leading and lagging modes. Here, r takes the values 0.00, 0.05, and 0.10. The tripping characteristic without SSSC is also plotted in dotted form.

It can be seen that as the injected voltage increases in the lagging mode, the measured resistance increases for the high fault resistances, while in the case of the low fault resistances, the measured resistance decreases; for zero fault resistance and high magnitudes of injected voltage, the measured resistance becomes negative. On the other hand, as the injected voltage increases, the measured reactance also increases. The increase in the measured reactance becomes greater for the higher fault resistances. Generally, it can be said that in the presence of SSSC in the lagging mode at the near end of the transmission line, the tripping characteristic expands and turns in anticlockwise direction.

It can be seen that as the injected voltage increases in the leading mode, the measured resistance changes complicatedly, it decreases for the high fault resistances, while in the case of the low fault resistances, the measured resistance increases. On the other hand, as the injected voltage increases, the measured reactance decreases. Generally, it can be said that in the presence of SSSC in the leading mode at the near end of the transmission line, the tripping characteristic shrinks and turns in clockwise direction.

5.2 VT in front of SSSC

In the case of SSSC, due to the absence of shunt branch, unit C_{1A} and C_{0A}, and equality of C_{ldf} and C_{ldb} to C_{ld}, both (40) and (41) are simplified as (43), the same as the case of TCSC.

Figure 12 shows the effect of an inactive SSSC presence on the line. It can be seen that even in the case of inactive SSSC the measured impedance is affected due to the presence of the coupling transformer in series with the line. The measured resistance increases, while the measured reactance decreases slightly. In the case of zero fault resistance, the measured impedance is the actual impedance of the line section between the relaying and fault points.

Figure 13 shows the effect of SSSC voltage magnitude variation on the measured impedance at the relaying point in the both leading and lagging modes. Here, r takes the values of 0.00, 0.05, and 0.10. The tripping characteristic without SSSC is also plotted in dotted form.

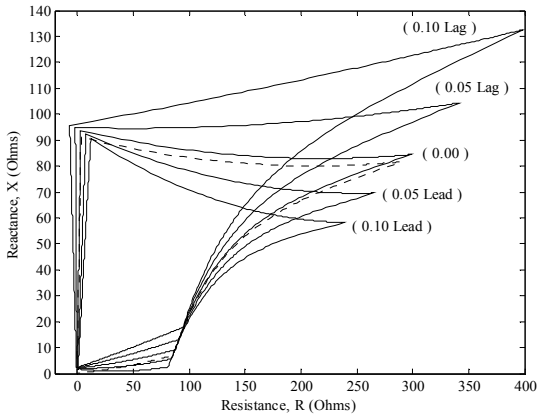

Fig. 11 Distance relay tripping characteristic variation; VT behind SSSC.

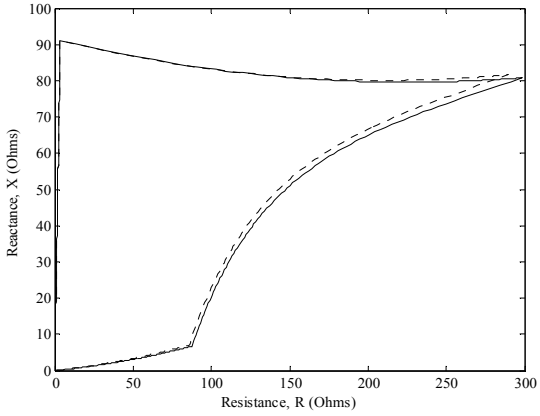

Fig. 12 Distance relay tripping characteristic; VT in front of SSSC, inactive SSSC.

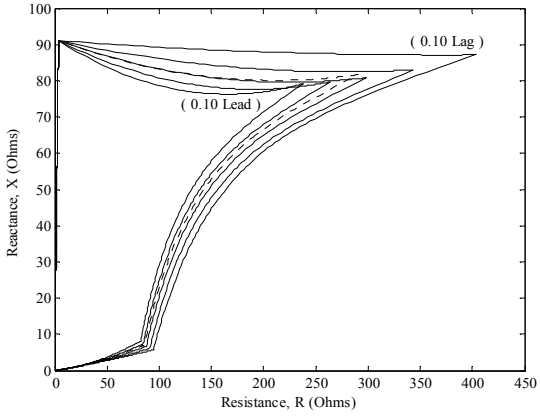

Fig. 13 Distance relay tripping characteristic variation; VT in front of SSSC.

It can be seen that as the injected voltage increases in the lagging mode, the measured resistance increases. On the other hand, as the injected voltage increases, the measured reactance also increases. The increase in the measured reactance becomes greater for the higher fault resistances. In the case of zero fault resistance, the measured impedance is the actual impedance of the line section between the relaying and fault points. Generally, it can be said that the tripping characteristic expands and no turning can be observed. It can be seen that as the injected voltage increases in the leading mode, the measured resistance decreases. On the other hand, as the injected voltage increases, the measured reactance changes complicatedly, it increases for the faults near the relaying point, but at the far end it increases for the high fault resistances, while in the case of the low fault resistances, it decreases. Generally, it can be said that in the presence of SSSC in the leading mode, the tripping characteristic shrinks and no turning could be observed.

6 Distance Relay Ideal Tripping Characteristic in Presence of UPFC

Due to the presence of the shunt branch in UPFC, unlike the cases of TCSC and SSSC, the connection points of both VT and CT are important. Therefore, four mentioned cases are studied.

6.1 VT behind, CT behind UPFC

In the case of UPFC, (38) is the measured impedance at the relaying point. Figure 14 shows the effect of an inactive UPFC presence on the line. Here, injected voltage of the series branch is zero and it does not inject or absorb any reactive power. The tripping characteristic without UPFC is also shown in dotted form.

It can be seen that in the presence of an inactive UPFC, the measured resistance increases for the high fault resistances, while in the case of the low fault resistances, the measured resistance decreases; for zero fault resistance and high magnitudes of injected voltage, the measured resistance becomes negative. On the other hand, the measured reactance increases. The tripping characteristic slightly transfers upward.

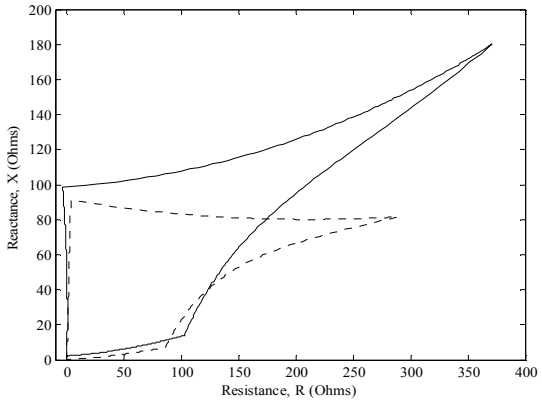

Fig. 14 Distance relay tripping characteristic; VT behind, CT behind UPFC, inactive UPFC.

Figure 15 shows the effect of UPFC controlling parameters variation on the measured impedance. Due to the various possible operational cases for UPFC, only four operational cases are considered. Here, $|E_{Sh}|$, r, and θ takes the values (1): (0.90,0.00,90), (2): (0.95,0.10,0), (3): (1.00,0.05,90), and (4): (1.05,0.10, –90).

It can be seen that as the controlling parameters of UPFC are varied, the tripping characteristic varies considerably. In the case of zero fault resistance, the measured impedance is not equal to the impedance of the line section between the relaying and fault points.

6.2 VT behind, CT in front of UPFC

In the case of UPFC, (39) is the measured impedance at the relaying point.

Figure 16 shows the effect of an inactive UPFC presence on the line. Here, injected voltage of the series branch is zero.

It can be seen that in the presence of an inactive UPFC, both the measured resistance and reactance increase slightly. The tripping characteristic slightly transfers upwards.

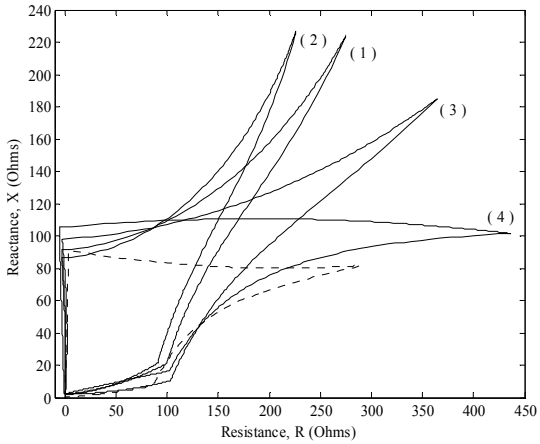

Fig. 15 Distance relay tripping characteristic variation; VT behind, CT behind UPFC.

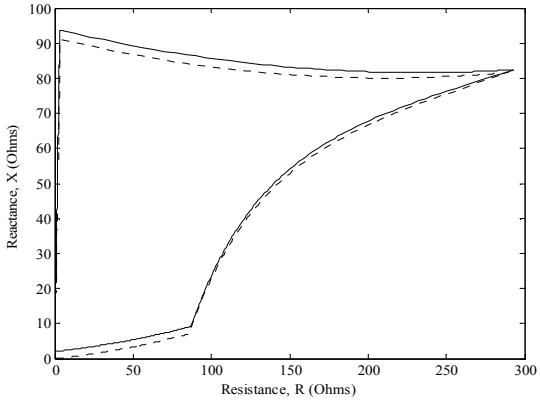

Fig. 16 Distance relay tripping characteristic; VT behind, CT in front of UPFC, inactive UPFC.

Figure 17 shows the effect of UPFC controlling parameters variation on the measured impedance. Here, $|E_{Sh}|$, r, and θ takes the values of mentioned cases of (1), (2), (3), and (4).

It can be seen that as the controlling parameters of UPFC are varied, the tripping characteristic varies considerably. In the case of zero fault resistance, the measured impedance is not equal to the impedance of the line section located between the relaying and the fault points, but its deviation is less than the previous case.

6.3 VT in front of, CT behind UPFC

In the case of UPFC, (40) is the measured impedance at the relaying point.

Figure 18 shows the effect of an inactive UPFC presence on the line. It can be seen that in the presence of an inactive UPFC the measured resistance increases for the high fault resistances, while in the case of the low fault resistances, the measured resistance decreases; for zero fault resistance and high magnitudes of injected voltage, the measured resistance becomes negative. On the other hand, the measured reactance also increases. In this case, no transfer of the tripping characteristic could be observed.

Figure 19 shows the effect of UPFC controlling parameters variation on the measured impedance. Here, $|E_{Sh}|$, r, and θ takes the values of mentioned cases of (1), (2), (3), and (4).

It can be seen that as the controlling parameters of UPFC are varied, the tripping characteristic varies considerably. In the case of zero fault resistance, the measured impedance is not equal to the impedance of the line section located between the relaying and fault points, but its deviation is less comparing with that of the first case.

6.4 VT in front of, CT in front of UPFC

In the case of UPFC, (41) represents the measured impedance at the relaying point.

Figure 20 shows the effect of an inactive UPFC presence on the line.

It can be seen that in the presence of an inactive UPFC the measured resistance increases slightly while the reactance decrease slightly. In this case no transfer of the tripping characteristic could be observed.

Figure 21 shows the effect of UPFC controlling parameters variation on the measured impedance. Here, $|E_{Sh}|$, r, and θ takes the values of mentioned cases of (1), (2), (3), and (4).

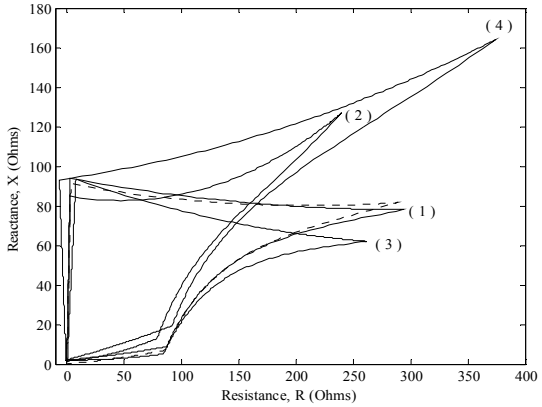

Fig. 17 Distance relay tripping characteristic variation; VT behind, CT in front of UPFC.

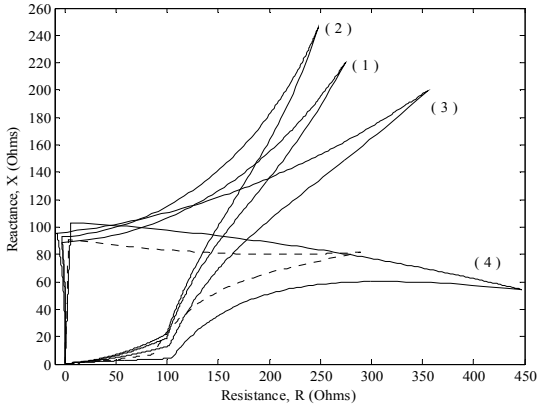

Fig. 19 Distance relay tripping characteristic variation; VT in front of, CT behind UPFC.

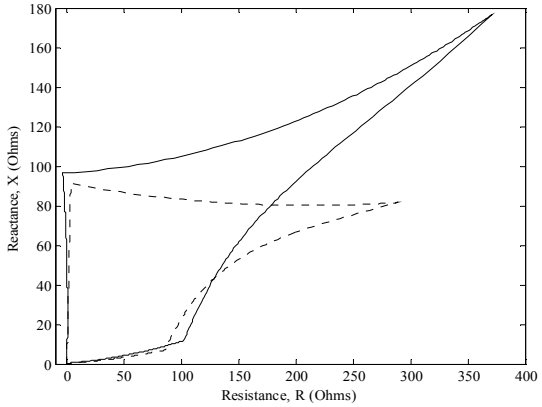

Fig. 18 Distance relay tripping characteristic; VT in front of, CT behind UPFC, inactive UPFC.

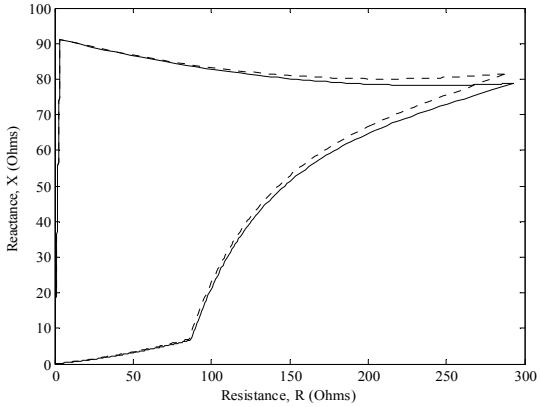

Fig. 20 Distance relay tripping characteristic; VT in front of, CT in front of UPFC, inactive UPFC.

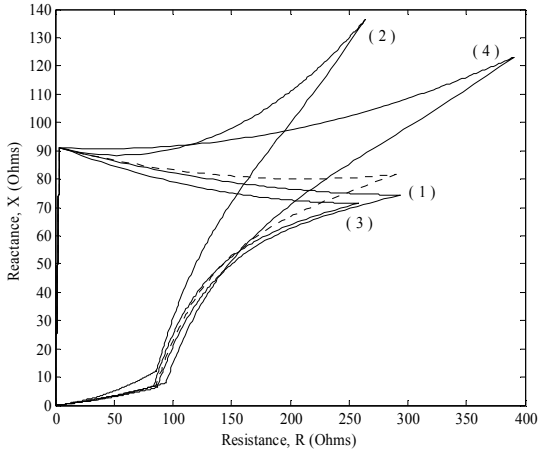

Fig. 21 Distance relay tripping characteristic variation; VT in front of, CT in front of UPFC.

It can be seen that as the controlling parameters of UPFC are varied, the tripping characteristic varies considerably. In the case of zero fault resistance, the measured impedance is equal to the actual impedance of the line section between the relaying and fault points.

7 Comparison

As mentioned, in the case of VT located behind TCSC, (42) indicates the measured impedance at the relaying point, whereas in the case of VT in front of TCSC, (43) presents this value. In the case of VT behind TCSC, the measured impedance at the relaying point deviates by two terms: $C_{1S}Z_{1L}$ which is added to pZ_{1L} leads to the tripping characteristic transfer downward or upward; and C_{Zse} which is due to the presence of TCSC impedance. In the case of compensation degree of zero, or inactive mode, the equivalent impedance of TCSC would be zero. Therefore, both terms would become zero and the tripping characteristic would be the same as the tripping characteristic without TCSC. Otherwise, two terms cause the transfer and the deviation, respectively. In the case of VT in front of TCSC, (43) represents the measured impedance which is the same as the measured impedance in absence of TCSC, (14), and two previously mentioned deviating terms are omitted. Here, there is no transfer. In the case of compensation degree of zero, inactive mode, the tripping characteristic would be the same as the tripping characteristic without TCSC. In other cases, there would be a deviation depending on TCSC compensation degree.

As mentioned, in the case of VT behind SSSC, (44) indicates the measured impedance at the relaying point. Here, the measured impedance at the relaying point deviates from its value without SSSC in three terms. First term is $C_{1S}Z_{1L}$, which is added to pZ_{1L} leads to the tripping characteristic transfer upward. Second term is C_{Zse}, which is due to the presence of the coupling transformer in series with the transmission line. Third term is C_{Vse}, which is due to the presence of the series voltage source in series with the transmission line. In the case of inactive SSSC, C_{Vse} is zero, but $C_{1S}Z_{1L}$, and C_{Zse} are not zero; therefore, the measured impedance deviates from its actual value. In the case of zero fault resistance, $C_{1S}Z_{1L}$, C_{Vse}, and C_{Zse} are not zero, so this leads to the measured impedance deviation.

In the case of VT in front of SSSC, (43) presents the measured impedance. Three previously mentioned deviating terms are omitted in this case. Here, no transfer or turning could be observed. For zero fault resistance, the measured impedance is the actual value.

As mentioned, in the case of VT behind and CT behind UPFC, (38) indicates the measured impedance at the relaying point. Here, the measured impedance at the relaying point deviates from its value without UPFC in four terms. First term is $C_{1S}Z_{1L}$, which is added to pZ_{1L} leads to the tripping characteristic transfer upward. Second term is C_{Sh}, which is due to the presence of the shunt branch. Third term is C_{Zse}, which is due to the presence of the coupling transformer in series with the transmission line. Fourth term is C_{Vse}, which is due to the presence of the series voltage source in series with the line. In the case of inactive UPFC, C_{Vse} is zero, but $C_{1S}Z_{1L}$, C_{Sh}, and C_{Zse} are not zero; therefore, the measured impedance deviates from its actual value. In the case of zero fault resistance, $C_{1S}Z_{1L}$, C_{Sh}, C_{Vse} and C_{Zse} are not zero, so this leads to the measured impedance deviation. In the case of VT behind and CT in front of UPFC, (39) indicates the measured impedance. Here, the measured impedance deviates from its value without UPFC in three terms: $C_{1S}Z_{1L}$, C_{Zse}, and C_{Vse}. In the case of inactive UPFC, C_{Vse} is zero, but $C_{1S}Z_{1L}$, and C_{Zse} are not zero; therefore, the measured impedance deviates from its actual value. In the case of zero fault resistance, $C_{1S}Z_{1L}$, C_{Vse}, and C_{Zse} are not zero, so the measured impedance deviates from its actual value. In the case of VT in front of and CT behind UPFC, (40) indicates the measured impedance. Here, the measured impedance deviates from its value without UPFC by two terms of $C_{1S}Z_{1L}$ and C_{Sh}. In the case of inactive UPFC, $C_{1S}Z_{1L}$ and C_{Sh} are not zero; therefore, the measured impedance deviates from its actual value. In the case of zero fault resistance, $C_{1S}Z_{1L}$ and C_{Sh} are not zero, so this leads to the measured impedance deviation. In the case of VT in front of and CT in front of UPFC, (41) presents the measured impedance. The previously mentioned deviating terms are omitted in this case. Here, no transfer or turning could be observed. In the case zero fault resistance, the measured impedance is the actual value.

8 Conclusions

The variation of the system conditions affects the tripping characteristic. The combination of the changes in the system conditions, FACTS devices structural and controlling parameters, and the distance relay instrument transformers connection points have a complicated influence on the measured impedance at the relaying point.

Comparing the various possible connection points of the distance relay instrument transformers, it could be observed that connecting these instrument transformers in front of FACTS devices leads to correct impedance measurement in the absence of the fault resistance.
Therefore, providing the voltage and current signals from voltage and current transformers in front of FACTS devices, leads to much more realistic operation of the protective relays for the faults in the first protective zone.

References

[1] Zhizhe Zh. and Deshu C., "An adaptive approach in digital distance protection," *IEEE Trans. Power Delivery*, Vol. 6, No. 1, pp. 135-142, Jan. 1991.

[2] Xia Y. Q., Li K. K., and David A. K., "Adaptive relay setting for stand-alone digital distance protection," *IEEE Trans. Power Delivery*, Vol. 9, No. 1, pp. 480-491, Jan. 1994.

[3] Jamali S., "A fast adaptive digital distance protection," in *Proc. 2001 IEE 7th International Conference on Developments in Power System Protection*, pp. 149-152.

[4] Dash P. K., Pradhan A. K., Panda G., and Liew A. C., "Adaptive relay setting for flexible AC transmission systems (FACTS)," in *Proc. 2000 IEEE Power Engineering Society Winter Meeting*, Vol. 3, pp. 1967-1972.

[5] Dash P. K., Pradhan A. K., Panda G., and Liew A. C., "Digital protection of power transmission lines in the presence of series connected FACTS devices," *IEEE Trans. Power Delivery*, Vol. 15, No. 1, pp. 38-43, Jan. 2000.

[6] Weiguo W., Xianggen Y., Jiang Y., Xianzhong D., and Deshu Ch., "The Impact of TCSC on Distance Protection Relay," in *Proc. 1998 IEEE International Conference on Power System Technology*, POWERCON'98, Vol. 1, pp. 382-388.

[7] Khederzadeh M., "The Impact of FACTS Devices on Digital Multifunction Protective Relays," in *Proc. 2002 IEEE Conference and Exhibition on Transmission and Distribution, Asia Pacific IEEE/PES*, Vol. 3, pp. 2043-2048.

[8] Dawei F., Chengxue Zh., Zhijian H., and Wei W., "The Effects of Flexible AC Transmission System Device on Protective Relay," in *Proc. 2002 IEEE International Conference on Power System Technology, POWERCON2002*, Vol. 4, pp. 2608-2611.

[9] Jamali S. and Shateri H., "Effects of Instrument Transformers Location on Measured Impedance by Distance Relay in Presence of TCSC," in *Proc. 8th IEE International Conference of AC and DC Transmission, ACDC 2006*, London, UK, 28-31 March 2006, pp. 9-13.

[10] Jamali S., Kalantar M., and Shateri H., "Effects of Instrument Transformers location on Measured Impedance by Distance Relay in Presence of UPFC," in *Proc. 2006 IEEE Power India Conference*, New Delhi, India, 10-12 April 2006.

[11] Kazemi A., Jamali S., and Shateri H., "Effects of Instrument Transformers Connection Point on Measured Impedance by Distance Relay in Presence of SSSC," in *Proc. 2006 International Conference on Power System Technology, POWERCON 2006*, Chongqing, China, 22-26 October 2006.

[12] Johns A. T., Ter-Gazarian A., and Warne D. F., "Flexible ac transmission systems (FACTS)," Padstow, Cornwall: TJ International Ltd., 1999.

[13] Jamali S. and Shateri H., "Robustness of distance relay with Quadrilateral characteristic against fault resistance," in *Proc. 2005 IEEE/PES Transmission and Distribution Conference and Exhibition: Asia and Pacific, IEEE/PES T&D 2005*.

[14] Dommel H. W., "EMPT reference manual," *Microtran Power System Analysis Corporation, Vancouver*, Canada, August 1997.

Hossein Shateri was born in 1979 in Karaj, Iran. He received his B.Sc. and M.Sc. from Iran University of Science and Technology in Tehran in 2001 and 2003, respectively all in Electrical Engineering. He is currently working towards a Ph.D. degree in the Department of Electrical Engineering at Iran University of Science and Technology (IUST) in Tehran, Iran since Sep. 2004. H. Shateri is a Member of the Institution of Electrical Engineers (IEE) and a Student Member of the Institution of Electrical and Electronic Engineers (IEEE). His field of interest includes Power System Protection, and Distribution Systems Protection and Automation.

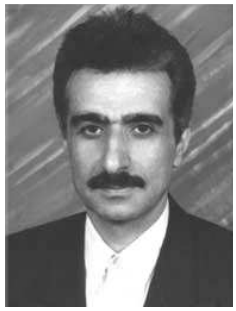

Sadegh Jamali was born in 1956 in Tehran, Iran. He received his B.Sc. from Sharif University of Technology in Tehran in 1979, M.Sc. from UMIST, Manchester, UK in 1986 and Ph.D. from City University, London, UK in 1990, all in Electrical Engineering. Dr. Jamali is currently an Associate Professor in the Department of Electrical Engineering at Iran University of Science and Technology in Tehran. Dr. Jamali is a Fellow of the Institution of Electrical Engineers (IEE) and the IEE Council Representative in Iran. His field of interest includes Power System Protection and Distribution Systems.